

Copper and nickel removal from plating wastewater in the electrodialysis process using a channeled stack

Kyung Jin Min^{1,2a}, Joo Hyeong Kim^{1b}, Sun Wouk Kim^{1b}, Seunghyun Lee^{1b},
Hyun-Gon Shin^{3c} and Ki Young Park^{*1}

¹Department of Civil and Environmental Engineering, Konkuk University, 120 Neungdong-ro, Gwangjin-gu, Seoul 05029, Korea

²Plagen Co. Ltd., 58 Wangsimni-ro, Seongdong-gu, Seoul 04778, Korea

³Department of Energy and Environmental Engineering, Shinhan University, Gyeonggi-do 480-857, Korea

(Received December 30, 2020, Revised April 27, 2021, Accepted May 3, 2021)

Abstract. Electrodialysis (ED) is an advanced separation process used to treat industrial wastewater using potential differences. In this study, flow rates within the stack were increased by creating a flow channel to increase the limiting current density (LCD). Increasing the flow rate within the stack increases the diffusion flux, which leads to an increase in LCDs. Experiments show that the applied voltage of the flow-accelerated stack was improved by 12.2% compared to the stack without a flow channel, but the LCD decreased by 3.6%. The removal efficiency of both copper and nickel between the two stacks was greater than 95.6%, with no significant difference. However, the concentration rate of ions was superior in the stack without a flow channel. This may be attributed to the fact that the applied voltage increases when the channel is attached, resulting in differences in the separation rate and the resulting concentration polarization. In terms of the current efficiency, the channel-less stack was found to be 42.5% better than the channeled stack. It would be desirable to apply voltages below the LCDs as those exceeding LCDs at the same membrane flow rate would significantly reduce the economic feasibility.

Keywords: channeled stack; current efficiency; economic feasibility; electrodialysis; limiting current density

1. Introduction

Organic and inorganic ions are present in most industrial and urban wastewater along with natural freshwater. In some cases, these ions need to be concentrated and recovered or completely removed (Zhang *et al.* 2012). High concentrations of various metals present in industrial wastewater can cause serious environmental pollution if not properly treated (Fu *et al.* 2011, Malamis *et al.* 2012). The electroplating industry wastewater contains various types of toxic substances such as cleaning agents, heavy metals, and solvents. Among these, metallic substances such as copper and nickel are dangerous, especially when discharged without treatment (Akbal and Camci 2011, Lee *et al.* 2017). Therefore, a variety of removal methods have been developed, including chemical precipitation/coagulation, membrane technology, electrolytic reduction, ion exchange, and adsorption (O'Connell *et al.* 2008).

Recently, ion exchange, reverse osmosis, nanofiltration, and electrodialysis (ED) have been proposed as technologies for the separation and concentration of ions (Strathmann 2010, Nakayama *et al.* 2017, La Cerva *et al.* 2018, Min *et al.* 2019, Oh *et al.* 2020). ED consists of

electrodes, spacers, and ion exchange membranes arranged in a way that has more than one separate stream. In ED, ions are separated by the potential differences of the two electrodes at either end of the ion exchange membrane system (Koutso *et al.* 2007, Silva *et al.* 2013, Iváñez Mengual *et al.* 2015). The rate of separation of ions depends on the charge and mobility of each ion, conductivity of the ionic solution, relative concentration of ions, and applied potential difference. Additionally, the results of ED also depend on the design parameters such as the flow rate, configuration, and structure of the cells and spacers (Lee *et al.* 2006, Silva *et al.* 2013, Min *et al.* 2020).

These parameters affect the current utilization and concentration polarization (Lee *et al.* 2002). Concentration polarization in ED occurs at the surface of the ion-exchange membrane. In general, the transport number of counter-ions is one and the transport number of co-ions is zero in ion-exchange membranes (Strathmann 2010). As the ion concentration in the ion exchange membrane is lower than that in the dilute, the ion concentration in the dilute solution decreases. Eventually, the electrolyte concentration at the membrane surface decreases, resulting in a concentration gradient between the membrane surface and well-mixed bulk fluid, resulting in the diffusion of electrolyte transport. A steady-state is obtained when the additional ions needed to balance those removed from the ion-exchange membrane surface are supplied by the diffusion transport. However, when the ion concentration of the dilute on the surface of the ion exchange membrane becomes zero, the current density approaches its maximum value, which is thus defined as the limiting current density

*Corresponding author, Ph.D., Professor,
E-mail: kypark@konkuk.ac.kr

^a Ph.D.

^b M.Sc. Student

^c Ph.D., Professor

(LCD) (Lee *et al.* 2006, Koutsou *et al.* 2007, Strathmann 2010). To maintain maximum efficiency without damaging the ion exchange membrane, a slightly higher current density than LCD must be supplied, but to prevent damage to the ion exchange membrane, a lower current density than LCD must be supplied. In addition, since energy consumption is determined by the current density, LCD is the most important design variable in terms of the economics and ion separation efficiency of the ED (Scarazzato *et al.* 2015, Jia *et al.* 2018).

Diffusion transport is closely related to the design parameters and the membrane surface flow rates. However, the increase in the flow rate on the membrane surface was minimized as the energy consumption increased. Thus, the geometry of the diluate and concentrate cells in the ED stack is created identically, in the same direction on a single surface to avoid both a linear streamline and a hydrostatic pressure difference. This resulted in a relatively low recovery rate of ED. The flow rate of the membrane could be increased by installing a channel in the stack of the ED to create a winding path flow. Consequently, as the path from the inlet to the outlet of the stack becomes longer, the flow rate quickens compared to a stack without channels (Strathmann 2010). A stack with a winding path flow is critical as it can increase treatment costs owing to high-pressure losses, but the flow rate in the stack increases the application efficiency (Veerman *et al.* 2011, Tedesco *et al.* 2012, Gurreri *et al.* 2012).

In this study, a stack with a long path narrowing towards the outlet was used, along with an increased flow rate, to apply a higher voltage while preventing concentration polarization. Since the cross-section of the flow path decreases as the width decreases in the direction of the outlet, the flow velocity in the stack increases as it reaches the outlet. As a result, since an increase in the flow velocity in the stack increases the ion transport rate to the surface of the ion exchange membrane, concentration polarization is prevented and a higher voltage (or current) can be applied, thereby improving the separation efficiency of ions.

The specific objectives of this study are to; (a) investigate the effect of the stacked channel on the LCD at the same flow rate, (b) compare the separation efficiency of copper and nickel ions in each LCD, and (c) evaluate the economy in terms of its current efficiency.

2. Materials and methods

2.1 Wastewater

Wastewater from an electroplating facility located in Ansan, Korea was used. The wastewater from the electroplating facility has a COD (chemical oxygen demand) of 963-998 mg/L (980 ± 15.2 mg/L), T-N (total nitrogen) of 1,475-1,505 mg/L ($1,490 \pm 11.3$ mg/L), and T-P (total phosphorus) of 5.8-6.2 mg/L (6.0 ± 1.8 mg/L). The copper and nickel concentrations were 1,582-1,612 mg/L ($1,596 \pm 9.38$ mg/L) and 260-273 mg/L (267 ± 4.0 mg/L), respectively, and the electrical conductivity was 18.4-19.0 mS/cm (18.6 ± 0.2 mS/cm), while the pH was 1.84-2.01 (1.98 ± 0.06).

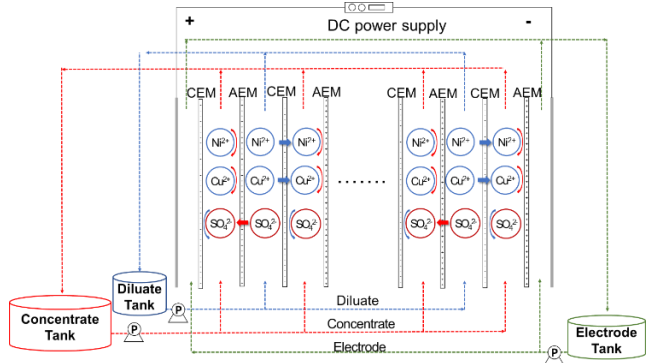
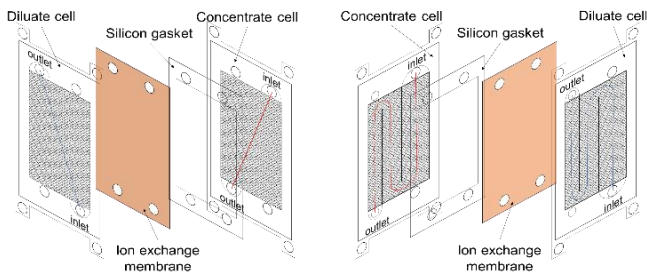


Fig. 1 Schematic illustrating electrodialysis



(a) Stack without channel (b) Stack with channel
Fig. 2 Schematic diagram illustrating the construction of a sheet flow stack design

2.2 Electrodialysis setup

The ED system consists of a PVC material diluate tank with a capacity of 0.5 L, concentrate and electrode solution tanks, three circulation pumps with a maximum flow rate of 7 L/min (NH-30PX, Pan world Co. Ltd., Korea). A standard laboratory apparatus consisting of a rectifier with an automatic control range of 0-30 V/0-3 A (P3030, Advantek Co. Ltd., Korea) was used. The size of each electrode installed at both ends of the stack was 45 mm (W) \times 105 mm (H) \times 2 mm (D). Each electrode consisted of a titanium base plated with a solution containing platinum and ruthenium to prevent corrosion. A schematic diagram of the device used in the experiment is shown in Fig. 1.

The size of the ion exchange stack used in the experiment was 115 mm (W) \times 225 mm (H). The effective area of the cation and the anion exchange membranes in the stack without channels is 55.5 cm^2 , and the total length of the flow path is 18 cm. Conversely, the effective area of the ion exchange membrane of the stack with channels is 48.5 cm^2 , and the total length of the flow path is 33.9 cm. A net-like spacer was installed in the diluate and concentrate cells of all stacks to induce a zigzag flow to provide a better turbulent flow and reduce the concentration polarization (Strathmann 2010, Min *et al.* 2021a, b). A schematic diagram of the stack used in the experiment is shown in Fig. 2.

In this study, Neosepta CMX-SB and AMX-SB from ASTOM (Tokyo, Japan) were used as cationic and anionic exchange membranes, respectively. Neosepta ion-exchange membranes are classified as homogeneous membranes because the bulk of the membrane, except for the

Table 1 Main properties of the ion exchange membrane

Type	Cationic (Neosepta CMX-SB)	Anionic (Neosepta AMX-SB)
Thickness (mm)	0.14 – 0.20	0.12 – 0.18
Burst strength (MPa)	≥ 0.40	≥ 0.25
Electric resistance at 0.5 M NaCl and 25°C (Ω cm ²)	2.0 – 3.5	2.0 – 3.5
Perselectivity 1.0/0.5 M KCl (%)	92	95
Ion exchange capacity (meq/g)	1.26 ± 0.05	1.30 ± 0.05
Water content (g H ₂ O/(g dry membrane))	-	0.10 – 0.14
Membrane density (g/cm ³)	-	1.10

reinforcing fabrics, contain no structural irregularities more than 1 μm (Pismenskaya *et al.* 2012, Mareev *et al.* 2018). It consists of randomly crosslinked sulfonated (CMX-SB) or aminated (AMX-SB) styrene-divinylbenzene copolymer (45–65%) and polyvinyl chloride (45–55%) (Mareev *et al.* 2018).

The ion exchange membrane was used in the experiment after immersion in the solution at 25 ± 1°C for 24 h. After the end of the experiment, the ion-exchange membrane was soaked in a solution containing 0.36% H₂SO₄ and 1.22% Na₂SO₄ (Sigma-Aldrich, USA) for 1 h to remove the precipitate attached to the surface. The physical properties of the ion exchange membrane are presented in Table 1 (Galvanin *et al.* 2016, Nebavskaya *et al.* 2017).

2.3 Operation conditions

The LCD was measured using wastewater with a concentration of 1,595 mg/L of Cu and 267 mg/L of Ni. The stack with and without channels consisted of five pairs of ion-exchange membranes. The potential increased by 1 V from 2 to 10 V, and subsequently increased by 2 V up to 20 V. The current and resistance were measured after stabilizing for 5 min in each step when applying a potential. As a difference exists in the effective area of each stack, the flow rate was adjusted to maintain the same flow rate of 1.44 cm/min at the membrane surface. The flow rate of the concentrate was kept the same as that of the membrane. Additionally, the removal efficiency of Cu and Ni was measured in a batch experiment under the LCD conditions determined in each stack. The electrolyte solution used 4% (w/w) Na₂SO₄ (Van de Bruggen *et al.* 2004, Ji *et al.* 2017). All experiments were conducted repeatedly.

2.4 Analytical methods

In all experiments, Orion 5 Star (Thermo Fisher Scientific Inc., USA), which can simultaneously measure the electrical conductivity and pH, was installed in the dilute and concentrate tanks, and measurements were conducted at 1-minute intervals. The current was measured at 1-minute intervals, and the resistance was calculated. Cu and Ni were sampled 5 min after the start of the experiment and collected every 10 min thereafter. The collected samples were filtered with a 0.45 μm syringe filter and subsequently measured according to EN ISO 11885:2007

using inductively coupled plasma optical emission spectroscopy (ICP-OES, ICP-6000, Thermo Fisher Scientific Inc., USA). The filtered sample was acidified with 2% HCl; more than six standard samples including the blank were prepared using a multi-element standard solution for ICP (Sigma-Aldrich Co., LLC., USA) to correct the calibration concentration. Samples with a concentration higher than the calibration concentration were measured by diluting with 2% HCl. The wavelengths of Ni and Cu were 231.60 nm and 324.75 nm, respectively (Min *et al.* 2021a, b).

The removal efficiency of heavy metals in the diluent during the ED operation was calculated as given by Eq. (1), and the recovery rate of heavy metals in the concentrated water was calculated as given by Eq. (2) (Wang *et al.* 2012).

$$\text{Removal efficiency (\%)} = \frac{C_o - C_t}{C_o} \times 100 \quad (1)$$

$$\text{Recovery rate (\%)} = \frac{C_t - C_0}{C_o} \times 100 \quad (2)$$

where C_o is the initial concentration of heavy metal ions before the experiment (mg/L) and C_t is the concentration of heavy metal ions at each experiment time interval (mg/L).

In the diluate tank containing the treated water of the ED process, the ion removal efficiency follows first-order kinetics at high concentrations, and after a certain time, this decreases to a zero-order reaction (Min *et al.* 2021a, b). Therefore, the change in electrical conductivity in the product over time is expressed as a shift order kinetic as given by Eq. (3).

$$\frac{k_1 C_t + k_2}{k_1 C_o + k_2} = e^{-k_1 t} \quad (3)$$

where C_o and C_t are the electrical conductivity (μS/cm) or ion concentration (mg/L) at the start of the experiment in the dilute and concentrate, respectively; at time t, k₁ and k₂ are first-order and zero-order constants, respectively.

Each stack is composed of five pairs, but as the charge passes through all the cell pairs connected in series, the current efficiency can be expressed as follows (Strathmann 2010, Wang *et al.* 2012, Min *et al.* 2021a, b).

$$\zeta = \frac{zFQC_s^\Delta}{IN} \quad (4)$$

where ζ is the efficiency of the current, I is the total current (A) applied to the stack, C_s^Δ is the difference in concentration (mol) between the feed and product solution, Z is the valence number of the ion, and F is the Faraday constant (C/mol). Q is the volumetric flow rate (m^3/s), and N is the total number of cell pairs.

3. Results and discussion

3.1 Limiting current density

LCD is the most important design factor determining the efficiency of ED, and various methods have been proposed for its accurate estimation (La Cerva *et al.* 2018). As the LCD depends on the fluid mechanics of the stack, structure of the flow channel, and spacer design, a method has been proposed to determine it using a mass transfer coefficient. The mass transfer coefficient can be determined by the Sherwood number, which is a function of the Schmidt and Reynolds numbers (Nikonenko *et al.* 2007, Ibáñez Mengual *et al.* 2014). However, it is difficult to directly determine the mass transfer coefficient in the ED stack as it must be measured independently (Lee *et al.* 2006). The most common way of determining the LCD is by using a current–voltage (V–I) curve determined through an experimental method (Lee *et al.* 2006).

Prior to all the experiments, the LCD in each stack was determined using an experimental method. In general, the LCD is determined through the inverse (1/A) of resistance and current, but differences in the LCD can occur depending on how the intersection is interpreted. Therefore, in this study, all the relationships between the voltage, resistance, and current are shown in Fig. 3. Using this method, the LCD can be determined to be low. However, considering the application of 70–90% of LCD (Silva *et al.* 2013) due to its economic feasibility in a full-scale facility, this method could intuitively determine the voltage and current. The LCD of the stack without channels was 4.32 A/m² and were calculated using the correlation between the voltage, resistance, and current; that for the stack with channels with increasing flow rate was 4.43 A/m². Compared to a stack without channels, LCDs in a high-flow rate stack with channels were improved by approximately 2.5%, but the limit voltages in both stacks were the same at 8 V. However, the LCDs calculated for the stack without channels using traditional V–I curves was 4.41 A/m², and that for the channeled stack was 4.25 A/m². The result of the V–I curve was calculated to be approximately 3.7% higher for the LCD of the stack without channels. However, the applied voltage for the stack without channels was the same at 8 V, but that for the channeled stack was 9 V. The LCD calculation using the V–I curve revealed that the high applied voltage of the channeled stack may be due to the increase in the flow rate in the stack when the flow rate in the stack reaches the outlet, along with the increase in the ion transport rate to the ion exchange membrane surface.

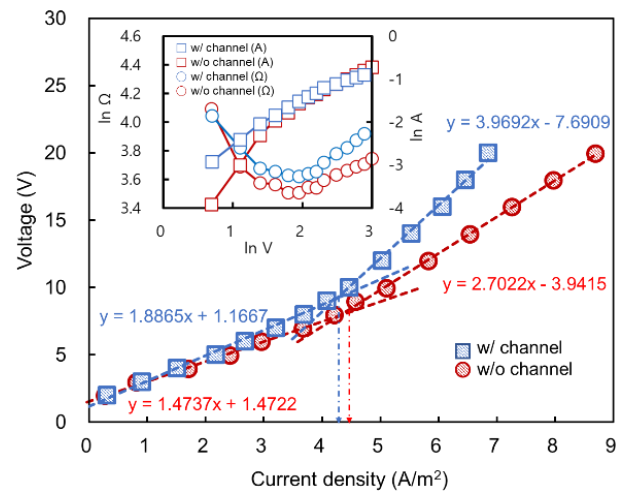


Fig. 3 Experimental LCD in each stack

3.2 Removal and recovery of ions

Based on the applied voltage of the LCD determined using the traditional V–I curves from the LCD experiment, the voltages of the channel-less and channeled stacks were 8 V and 9 V, respectively. For safety purposes, a potential difference voltage mode was applied as very low concentrations of dilute could produce high voltages in the ion exchange membrane stack (Gherasim *et al.* 2014). During the ED process, the ion removal efficiencies and concentration rates were estimated through the regression analysis of the analytical experimental data. Fig. 4 shows the changes in the electrical conductivity of the dilute and the concentrate over time in each stack. The ion removal efficiencies and concentration rates of the channeled stack are faster than that of the channel-less stack. This difference may be due to the difference in the applied voltage as the driving force of ions passing through the ion exchange membrane is proportional to the electric field strength (Káňová and Machuča 2014).

Increasing the applied voltage increases the rate of ion transfer through the membrane; thus, ion separation may occur rapidly in the early stages of the ED operation. The ion separation rate of the channeled stack was high up to 20 min after the experiment; however, the ion separation rate of the channel-less stack was higher thereafter. This difference in the ion separation rate can be confirmed by the ion removal efficiency. Until the initial 20 min of the experiment, the ion removal efficiencies of the channel-less and channeled stacks were 91.4% and 92.2%, respectively, but the final removal efficiencies were 97.3% and 96.8%, respectively. The rate constant generally increases as the applied voltage increases and begins to decrease after reaching a maximum value. This decrease in the rate constant is related to the ionic concentration of the solution and the ionic resistance of the membrane. The increase in the ionic resistance of the membrane with the decrease in the concentration of ions may be due to the concentration polarization or diffusion boundary layer resistance (Geise *et al.* 2014). As the flow rate of the stacks is the same, the effect of concentration polarization will be predominant

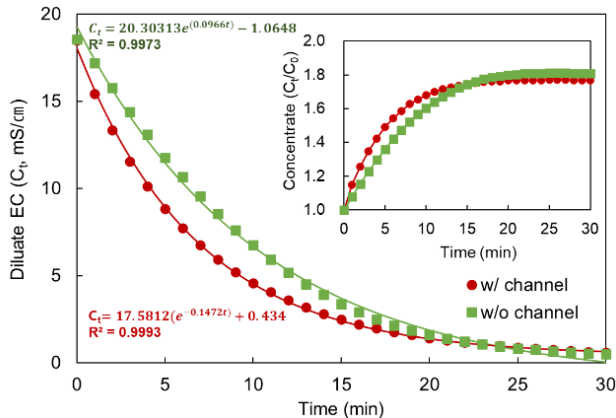
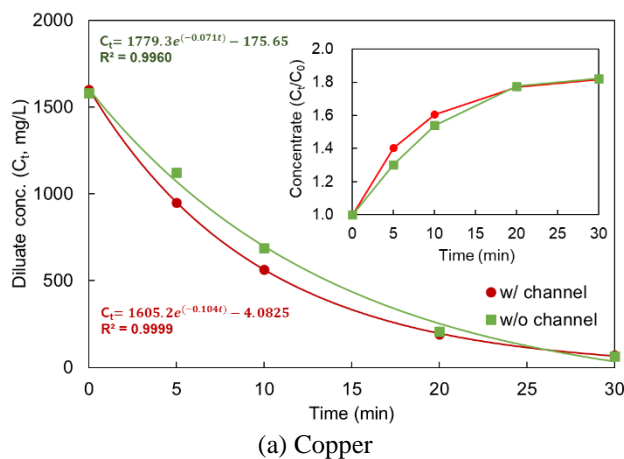
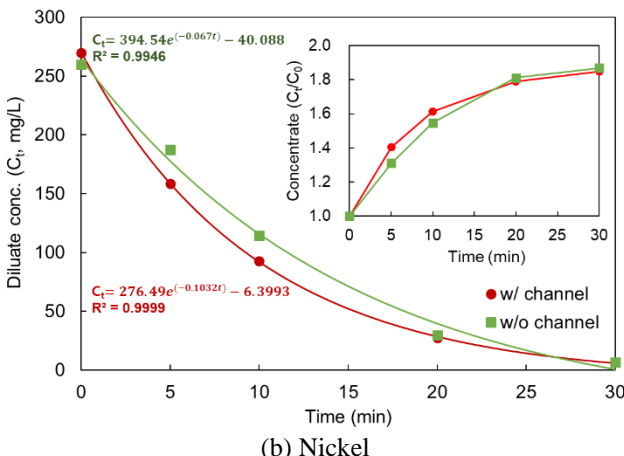


Fig. 4 Changes in the electrical conductivity of the diluate and concentrate in each stack



(a) Copper



(b) Nickel

Fig. 5 Changes in the copper and nickel concentrations in the diluate and concentrate water in each stack

rather than that of the diffusion boundary layer. As the channeled stack decreased the concentration of ions quickly due to the higher applied voltage, the influence on the concentration polarization during the total experiment time would be greater than that of the channel-less stack. Although there is a difference in the removal efficiency of ions, the final ion concentration rates of the channel-less and channeled stacks were 81.2% and 81.3%, respectively. Thus, no significant difference was observed.

The removal efficiencies of copper and nickel were better in the channeled stack (Fig. 5). Although the removal efficiency of nickel was slightly higher than that of copper in each stack, no significant difference was observed in the removal efficiency as both copper and nickel are divalent ions (Zhang *et al.* 2017).

The efficiency of copper removal between the two stacks was approximately the same. Furthermore, the removal efficiency of copper was 95.6 and 95.8% for channel-less and channeled stacks, respectively, showing no significant differences. The nickel removal efficiency of the channeled stack was slightly higher than that of the channel-less stack. However, the removal efficiencies of the channel-less and channeled stacks were 97.4 and 97.5%, respectively, with no significant differences between the stacks, as observed with copper. However, the channel-less stack showed a better recovery rate. For copper, the recovery rate of the channel-less stack was 82.2%, and that of the channeled stack was 81.7%. In the case of nickel, the recovery rates of the channel-less and channeled stacks were 86.8 and 84.8%, respectively. This difference may be due to the low applied voltage of the channel-less stack, which reduced the concentration polarization compared to the channeled stack. Therefore, considering the removal efficiency of ions, it may be effective to operate lower than the limiting current density.

In wastewater with a low concentration of copper and nickel, concentration polarization occurs more quickly, which can lead to significant differences in ion removal efficiency. Therefore, so further studies on the optimal operating conditions are required.

3.3 Current efficiency

The required membrane area can be calculated using the current density, feed and product concentration, flow rate, and current efficiency, as shown by Eq. (4). The maintenance cost of the ED process is classified into the labor, maintenance, and energy costs, and is generally calculated using proportional constants as it is directly proportional to the production capacity. The economic feasibility of an ED plant is calculated as the sum of the facility and energy costs (Starthmann 2010). The energy required in the ED process can be divided into the electrical energy required to concentrate the ionic component of the feed into a concentrated solution and the energy required to supply and circulate the solution to the stack (Bernardes *et al.* 2016). As LCD is inversely proportional to the membrane area, the capital cost decreases with increasing LCD, but with the increase in the maintenance cost. Additionally, as LCD affects the lifetime of the membrane, the economic feasibility can be ensured only by operating the facility considering the current efficiency.

The current efficiency under each experimental condition increased 10 min after the start of the experiment but subsequently decreased significantly as the operating time increased (Fig. 6). The current efficiency of the channel-less stack was better than that of the channeled stack. During the initial 10 min, the current efficiency of the channel-less stack was 5% better than that of the channeled

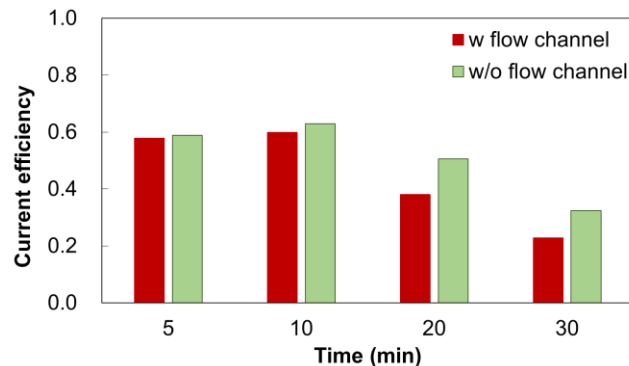


Fig. 6 Current efficiency over the operating time of each stack

stack, and the final current efficiency was 42.5% better. This is because the voltage of the channeled stack was 12.5% higher than that of the channel-less stack at the same membrane surface flow rate, but the final ion removal efficiency was 0.51% lower. During the ED, the diffusion flux in the ion exchange membrane is proportional to the ion concentration in the feed water. As the concentration of dilute decreases over the operation time, the diffusion flux decreases, and the concentration polarization occurs on the surface of the ion exchange membrane, increasing the electrical resistance (Bernards *et al.* 2016). Therefore, applying a voltage exceeding the LCD at the same membrane surface flow rate can decrease the efficiency of the current and increase the energy cost; therefore, applying a voltage below the LCD is desirable.

4. Conclusions

In this study, to increase the LCD and prevent concentration polarization, a channeled stack with a long path and a stack without a channel were compared. Consequently, the LCD obtained by the traditional V-I curve of the channel-less stack was higher than that of the channeled stack at the same membrane flow rate. However, the applied voltage was higher in the channeled stack because the flow rate of the channeled stack increased towards the outlet, along with the increased ion transport rate to the surface of the ion exchange membrane compared to the channel-less stack. Considering the ion removal efficiency, the ion separation rate of the channeled stack, to which a high voltage was applied, was fast at the start of the experiment. However, as the concentration of ions decreased quickly, the concentration polarization occurred earlier, eventually slowing down the ion separation rate. Therefore, the final removal efficiency was also lower than that of the channel-less stack. In particular, the high applied voltage had a greater effect on the concentrate rate of ions due to the concentration polarization. There was almost no difference in the removal efficiency of copper and nickel depending on the presence of channels, but the concentration of ions was high due to the reduced effect of the concentration polarization in the channel-less stack wherein the applied voltage was low. The current efficiency

in both stacks decreased with increasing operating time. In particular, the current efficiency of the channeled stack was considerably low compared to the channel-less stack because the concentration polarization phenomenon occurred faster, and the applied voltage was high. However, as the current efficiency of the channel-less stack was also considerably low, operating below LCDs would be desirable for the cost.

Acknowledgments

This study was supported by the Konkuk University Researcher Fund in 2020. This research was financially supported by the Korea Ministry of Environment as Waste to Energy-Recycling Human Resource Development Project and the Human Resource Program (Grant No. 20194010201790) of the Korea Institute of Energy Technology Evaluation and Planning (KETEP) grant funded by the Ministry of Trade, Industry & Energy (MOTIE) of the Republic of Korea.

References

- Akbal, F. and Camci, S. (2011), "Copper, chromium and nickel removal from metal plating wastewater by electrocoagulation", *Desalination*, **269**(1-3), 214-222. <https://doi.org/10.1016/j.desal.2010.11.001>.
- Bernardes, A.M., Rodrigues, M.A.S. and Ferreira J.Z. (2016), *Electrodialysis and Water Reuse*, (1st Edition), Springer-Verlag, Berlin, Germany.
- Fu, F. and Wang, Q. (2011), "Removal of heavy metal ions from wastewaters: A review", *J. Environ. Manage.*, **92**, 407-418. <https://doi.org/10.1016/j.jenvman.2010.11.011>.
- Galvanin, F., Marchesini, R., Barolo, M., Bezzo, F. and Fidaleo, M. (2016). "Optimal design of experiments for parameter identification in electrodialysis models", *Chem. Eng. Res. Des.*, **105**, 107-119. <https://doi.org/10.1016/j.cherd.2015.10.048>.
- Geise, G.M., Curtis, A.J., Hatzell, M.C., Hickner, M.A. and Logan, B.E. (2014), "Salt concentration differences alter membrane resistance in reverse electrodialysis stacks", *Environ. Sci. Technol.*, **1**(1), 36-39. <https://doi.org/10.1021/ez4000719>.
- Gherasim, C.V., Krivcik, J. and Mikulašek, P. (2014), "Investigation of batch electrodialysis process for removal of lead ions from aqueous solutions", *Chem. Eng. J.*, **256**(15), 324-334. <https://doi.org/10.1016/j.cej.2014.06.094Get>.
- Gurrieri, L., Tamburini, A., Cipollina, A. and Micale, G. (2012), "CFD analysis of the fluid flow behavior in a reverse electrodialysis stack", *Desalin. Water Treat.*, **48**(1), 390-403. <https://doi.org/10.1080/19443994.2012.705966>.
- Ibáñez Mengual, J.A., Valerdi Pérez, R. and Carbonell Bejerano, F. (2015), "Characterization of an electrodialytic cell: Automation and process control", *Desalin. Water Treat.*, **56**(13), 3654-3664. <https://doi.org/10.1080/19443994.2014.991947>.
- Ji, Z.Y., Chen, Q.B., Yuan, J.S., Liu, J., Zhao, Y.Y. and Feng, W.X. (2017), "Preliminary study on recovering lithium from high Mg²⁺/Li⁺ ratio brines by electrodialysis", *Sep. Purif. Technol.*, **172**, 168-177. <https://doi.org/10.1016/j.seppur.2016.08.006>.
- Jia, Y.X., Li, F.J., Chen, X. and Wang, M. (2018), "Model analysis on electrodialysis for inorganic acid recovery and its experimental validation", *Sep. Purif. Technol.*, **190**, 261-267.

- <https://doi.org/10.1016/j.seppur.2017.08.067>.
- Káňavová, N. and Machuča, L. (2014), "A novel method for limiting current calculation in electrodialysis modules", *Period. Polytech. Chem. Eng.*, **58**(2), 125-130.
<https://doi.org/10.3311/PPCh.7145>.
- Koutsou, C.P., Yiantzios, S.G. and Karabelas, A.J. (2007), "Direct numerical simulation of flow in spacer-filled channels: Effect of spacer geometrical characteristics", *J. Membr. Sci.*, **291**(1-2), 53-69. <https://doi.org/10.1016/j.memsci.2006.12.032>.
- La Cerva, M., Gurreri, L., Tedesco, M., Cipollina, A., Ciofalo, M., Tamburini, A. and Micale, G. (2018), "Determination of limiting current density and current efficiency in electrodialysis units", *Desalination*, **445**, 138-148.
<https://doi.org/10.1016/j.desal.2018.07.028>.
- Lee, H.J., Strathmann, H. and Moon, S.H. (2006), "Determination of the limiting current density in electrodialysis desalination as an empirical function of linear velocity", *Desalination*, **190**, 43-50. <https://doi.org/10.1016/j.desal.2005.08.004>.
- Lee, C.G., Lee, S., Park, J.A., Park, C., Lee, S.J., Kim, S.B., An, B., Yun, S.T., Lee, S.H. and Choi, J.W. (2017), "Removal of copper, nickel and chromium mixtures from metal plating wastewater by adsorption with modified carbon foam", *Chemosphere*, **166**, 203-211.
<https://doi.org/10.1016/j.chemosphere.2016.09.093>.
- Lee, H., Sarfert, F., Strathmann, H. and Moon, S. (2002), "Designing of an electrodialysis desalination plant", *Desalination*, **142**, 267-286.
[https://doi.org/10.1016/S0011-9164\(02\)00208-4](https://doi.org/10.1016/S0011-9164(02)00208-4).
- Malamis, S., Katsou, E., Kosanovic, T. and Haralambous, K.J. (2012), "Combined adsorption and ultrafiltration processes employed for the removal of pollutants from metal plating wastewater", *Sep. Sci. Technol.*, **47**(7), 983-996.
<https://doi.org/10.1080/01496395.2011.645983>.
- Mareev, S.A., Butylskii, D.Y., Pismenskaya, N.D., Larchet, C., Dammak, L. and Nikonenko, V.V. (2018), "Geometric heterogeneity of homogeneous ion-exchange Neosepta membranes", *J. Membr. Sci.*, **563**, 768-776.
<https://doi.org/10.1016/j.memsci.2018.06.018>.
- Min, K.J., Choi, S.Y., Jang, D., Lee, J. and Park, K.Y. (2019), "Separation of metals from electroplating wastewater using electrodialysis", *Energ. Source Part A*, **41**(20), 2471-2480.
<https://doi.org/10.1080/15567036.2019.1568629>.
- Min, K.J., Oh, E.J., Kim, G., Kim, J.H., Ryu, J.H. and Park, K.Y. (2020), "Influence of linear flow velocity and ion concentration on limiting current density during electrodialysis", *Desalin. Water Treat.*, **175**, 334-340.
<https://doi.org/10.5004/dwt.2020.24663>.
- Min, K.J., Kim, J.H. and Park, K.Y. (2021a), "Characteristics of heavy metal separation and determination of limiting current density in a pilot-scale electrodialysis process for plating wastewater treatment", *Sci. Total Environ.*, **757**, 143762.
<https://doi.org/10.1016/j.scitotenv.2020.143762>.
- Min, K.J., Kim, J.H., Oh, E.J., Ryu, J.H. and Park, K.Y. (2021b), "Flow velocity and cell pair number effect on current efficiency in plating wastewater treatment through electrodialysis", *Environ. Eng. Res.*, **26**(2), 190502.
<https://doi.org/10.4491/eer.2019.502>.
- Nakayama, A., Sano, Y., Bai, X. and Tado, K. (2017), "A boundary layer analysis for determination of the limiting current density in an electrodialysis desalination", *Desalination*, **404**, 41-49. <https://doi.org/10.1016/j.desal.2016.10.013>.
- Nebavskaya, K.A., Sarapulova, V.V., Sabbatovskiy, K.G., Sobolev, V.D., Pismenskaya, N.D., Sistat, P., Cretin, M. and Nikonenko, V.V. (2017), "Impact of ion exchange membrane surface charge and hydrophobicity on electroconvection at underlimiting and overlimiting currents" *J. Membr. Sci.*, **523**, 36-44. <https://doi.org/10.1016/j.memsci.2016.09.038>.
- Nikonenko, V.V., Pis'menskaya, N.D., Istoshin, A.G., Zabolotskii, V.I. and Shudrenko, A.A. (2007), "Generalization and prognostication of mass exchange characteristics of electrodialyzers operating in overlimiting current regimes with use made of similarity theory and compartmentation method", *Russ. J. Electrochem.*, **43**(9), 1069-1081.
<https://doi.org/10.1134/S102319350709011X>.
- O'Connell, D.W., Birkinshaw, C. and O'Dwyer, T.F. (2008), "Heavy metal adsorbents prepared from the modification of cellulose: A review", *Bioresource Technol.*, **99**(15), 6709-6724.
<https://doi.org/10.1016/j.biortech.2008.01.036>.
- Oh, E., Kim, J., Ryu, J.H., Min, K.J., Shin, H.G. and Park, K.Y. (2020), "Influence of counter anions on metal separation and water transport in electrodialysis treating plating wastewater", *Membr. Water Treat.*, **11**(3), 201-206.
<http://doi.org/10.12989/sem.2020.11.3.201>.
- Pismenskaya, N.D., Nikonenko, V.V., Melnik, N.A., Shevtsova, K.A., Belova, E.I., Pourcelly, G., Cot, D., Dammak, L. and Larchet, C. (2012), "Evolution with time of hydrophobicity and microrelief of a cation-exchange membrane surface and its impact on over-limiting mass transfer", *J. Phys. Chem. B*, **116**, 2145-2161. <https://doi.org/10.1021/jp2101896>.
- Scarazzato, T., Buzzi, D.C., Bernardes, A.M., Tenório, J.A.S. and Espinosa, D.C.R. (2015), "Current-voltage curves for treating effluent containing HEDP: Determination of the limiting current", *Braz. J. Chem. Eng.*, **32**(4), 831-836.
<https://doi.org/10.1590/0104-6632.20150324s00003511>.
- Silva, V., Poiesz, E. and Van der Heijden, P. (2013), "Industrial wastewater desalination using electrodialysis: Evaluation and plant design", *J. Appl. Electrochem.*, **43**(11), 1057-1067.
<https://doi.org/10.1007/s10800-013-0551-4>.
- Strathmann, H. (2010), "Electrodialysis, a mature technology with a multitude of new applications", *Desalination*, **264**(3), 268-288. <https://doi.org/10.1016/j.desal.2010.04.069>.
- Tedesco, M., Cipollina, A., Tamburini, A., van Baak, W. and Micale, G. (2012), "Modelling the Reverse ElectroDialysis process with seawater and concentrated brines", *Desalin. Water Treat.*, **49**(1), 404-424.
<https://doi.org/10.1080/19443994.2012.699355>.
- Van der Bruggen, B., Koninckx, A. and Vandecasteele, C. (2004), "Separation of monovalent and divalent ions from aqueous solution by electrodialysis and nanofiltration", *Water Res.*, **38**(5), 1347-1353. <https://doi.org/10.1016/j.watres.2003.11.008>.
- Veerman, J., Saakes, M., Metz, S.J. and Harmsen, G.J. (2011), "Reverse electrodialysis: A validated process model for design and optimization", *Chem. Eng. J.*, **166**(1), 256-268.
<https://doi.org/10.1016/j.cej.2010.10.071>.
- Wang, X., Nie, Y., Zhang, X., Zhang, S. and Li, J. (2012), "Recovery of ionic liquids from dilute aqueous solutions by electrodialysis", *Desalination*, **285**, 205-212.
<https://doi.org/10.1016/j.desal.2011.10.003>.
- Zhang, Y., Paepen, S., Pinoy, L., Meesschaert, B. and Van der Bruggen, B. (2012), "Selectrodialysis: Fractionation of divalent ions from monovalent ions in a novel electrodialysis stack", *Sep. Purif. Technol.*, **88**, 191-201.
<https://doi.org/10.1016/j.seppur.2011.12.017>.
- Zhang, Y.H., Liu, F.Q., Zhu, C.Q., Zhang, X.P., Wei, M.M., Wang, F.H., Ling, C. and Li, A.M. (2017). "Multifold enhanced synergistic removal of nickel and phosphate by a (N, Fe)-dual-functional bio-sorbert: Mechanism and application", *J. Hazard. Mater.*, **329**, 290-298.
<https://doi.org/10.1016/j.jhazmat.2017.01.054>.